natural mechanism of aggregation.

The problem of the optimal path, for which C_m is a minimum, has been solved exactly in two dimensions in the context of domain walls in random ferromagnets and directed polymers in a random medium (*16*). The Hurst exponent $H = \frac{2}{3}$. For directed, self-affine river basins, the values of τ and h can readily be deduced to be $\frac{7}{5}$ and $\frac{3}{5}$, respectively. These values are robust and do not change even if the minimization of the energy functional includes both directed and undirected networks (*16*).

For $\frac{1}{2} \leq \gamma < 1$, heterogeneities in the erosional properties are irrelevant, and the exponent values are the same as their homogeneous counterparts. Our proof relies on first observing that Min $E \leq L^{1+2\gamma}$ (Min $E \leq \Sigma_i k_i s_i^\gamma$ for the tree for which $\Sigma_i s_i^\gamma$ is a minimum, but $\Sigma_i k_i s_i^\gamma \leq k_i^{\max} \Sigma_i s_i^\gamma \approx k_i^{\max} L^{1+2\gamma}$, where $k_i^{\max}$ is the largest of the k_i values) and then using Eq. 9 in conjunction with Eq. 3 to show that $H \geq 1$. Because $H > 1$ is not physically meaningful, the Hurst exponent remains unchanged at $H = 1$.

We have thus shown that OCNs with $\frac{1}{2} \leq \gamma \leq 1$ show three classes of behavior (Table 1). Our results indicate that the OCN, in its present form, does not describe the behavior of river basins. Rinaldo and co-workers (*6*) have carried out numerical studies of the $\gamma = \frac{1}{2}$ case. Their work, which was restricted to the statistics of local minima (and not the global minimum, as in our analysis), yielded exponents different from our results but in good accord with observational data.

REFERENCES AND NOTES

1. I. Rodriguez-Iturbe, R. L. Bras, E. Ijjasz-Vasquez, D. G. Tarboton, *Water Resour. Res.* **28**, 988 (1992); D. G. Tarboton, R. L. Bras, I. Rodriguez-Iturbe, *ibid.* **24**, 1317 (1988); *ibid.* **26**, 2243 (1990); P. La Barbera and R. Rosso, *ibid.* **25**, 735 (1989); S. P. Breyer and R. S. Snow, *Geomorphology* **5**, 143 (1992); D. R. Montgomery and W. E. Dietrich, *Science* **255**, 826 (1992); D. G. Tarboton, R. L. Bras, I. Rodriguez-Iturbe, *Water Resour. Res.* **25**, 2037 (1989).
2. R. E. Horton, *Geol. Soc. Am. Bull.* **56**, 275 (1945); *Eos* **13**, 350 (1932).
3. R. L. Shreve, *J. Geol.* **74**, 17 (1966); *ibid.* **75**, 178 (1967); *ibid.* **77**, 397 (1969).
4. L. B. Leopold and W. B. Langbein, *U.S. Geol. Surv. Prof. Pap. 500-A* (1962).
5. A. D. Howard, *Water Resour. Res.* **26**, 2107 (1990); *ibid.* **7**, 863 (1971); C. T. Yang, *ibid.*, p. 311; P. S. Stevens, *Patterns in Nature* (Little-Brown, Boston, MA, 1974).
6. I. Rodriguez-Iturbe, A. Rinaldo, R. Rigon, R. L. Bras, E. Ijjasz-Vasquez, *Water Resour. Res.* **28**, 1095 (1992); *Geophys. Res. Lett.* **19**, 889 (1992); A. Rinaldo, I. Rodriguez-Iturbe, R. Rigon, E. Ijjasz-Vasquez, R. L. Bras, *Phys. Rev. Lett.* **70**, 822 (1993); I. Rodriguez-Iturbe and A. Rinaldo, *Fractal River Basins: Chance and Self-Organization* (Cambridge Univ. Press, Cambridge, 1996); see also P. Yam, *Sci. Am.* **271**, 26 (November 1994).
7. T. Sun, P. Meakin, T. Jøssang, *Phys. Rev. E* **49**, 4865 (1994); *ibid.* **51**, 5353 (1995); *Water Resour. Res.* **30**, 2599 (1994); P. Meakin, J. Feder, T. Jøssang, *Physica A* **176**, 409 (1991).
8. The effects of evaporation of the water are captured by a negative contribution to R_i. It can be shown that randomness in R_i does not change the universality class.
9. A. E. Scheidegger, *Bull. Int. Assoc. Sci. Hydrol.* **12**, 15 (1967).
10. H. Takayasu, M. Takayasu, A. Provata, G. Huber, *J. Stat. Phys.* **65**, 725 (1991).
11. A. Maritan, A. Rinaldo, R. Rigon, I. Rodriguez-Iturbe, A. Giacometti, *Phys. Rev. E* **53**, 1501 (1996).
12. Our finite-size scaling arguments and the notion of universality are similar to those in critical phenomena. See, for example, M. E. Fisher, *Rev. Mod. Phys.* **46**, 597 (1974).
13. Directed networks are ones in which there is no local flow with a component away from the dominant flow direction. Generally, the mean area $\langle s \rangle$ scales as L^{d_f}, where the fractal dimension of the stream $d_f \geq 1$. The fractal situation $d_f > 1$ corresponds to $H = 1$, whereas a self-affine geometry has $d_f = 1$ and $H \leq 1$. All of our results hold for arbitrary networks without any restriction on their directedness.
14. J. T. Hack, *U.S. Geol. Surv. Prof. Paper 294-B* (1957). The principal cause of the anomalous exponent of Hack is a matter of debate. Basin elongation occurs in the Scheidegger model (*9*, *10*), but this model is yet untested with large sets of data. Alternately, computer simulations (*7*) suggest that basin shapes have a similarity across scales.
15. This substitution is a generalization of the observation that the mean area is equal to the average distance to the outlet [B. M. Troutman and M. R. Karlinger, *Water Resour. Res.* **28**, 563 (1992), and references therein].
16. D. A. Huse and C. L. Henley, *Phys. Rev. Lett.* **54**, 7708 (1985); M. Kardar, *ibid.* **55**, 2923 (1985); D. A. Huse, C. L. Henley, D. S. Fisher, *ibid.*, p. 2924.

17. We are indebted to A. Giacometti and I. Rodriguez-Iturbe and especially to A. Rinaldo for numerous stimulating discussions. This work was supported by grants from the Komitet Badan Naukowych, the National Aeronautics and Space Administration, the North Atlantic Treaty Organization, the National Science Foundation, and the Petroleum Research Fund administered by the American Chemical Society.

17 November 1995; accepted 7 March 1996

Predatory Dinosaurs from the Sahara and Late Cretaceous Faunal Differentiation

Paul C. Sereno,* Didier B. Dutheil, M. Iarochene, Hans C. E. Larsson, Gabrielle H. Lyon, Paul M. Magwene, Christian A. Sidor, David J. Varricchio, Jeffrey A. Wilson

Late Cretaceous (Cenomanian) fossils discovered in the Kem Kem region of Morocco include large predatory dinosaurs that inhabited Africa as it drifted into geographic isolation. One, represented by a skull approximately 1.6 meters in length, is an advanced allosauroid referable to the African genus *Carcharodontosaurus*. Another, represented by a partial skeleton with slender proportions, is a new basal coelurosaur closely resembling the Egyptian genus *Bahariasaurus*. Comparisons with Cretaceous theropods from other continents reveal a previously unrecognized global radiation of carcharodontosaurid predators. Substantial geographic differentiation of dinosaurian faunas in response to continental drift appears to have arisen abruptly at the beginning of the Late Cretaceous.

Major continental areas became increasingly isolated during the Late Cretaceous as non-avian dinosaurs underwent their final radiation. The influence of continental fragmentation on dinosaur evolution during this interval has remained uncertain because of uneven sampling of the fossil record. Late Cretaceous dinosaurian remains have been recovered principally from Asia and western North America and consist largely of coelurosaurian predators and ornithischian herbivores (*1*). Although dinosaur bones of Late Cretaceous age have been reported from all major southern land areas including Antarctica (*2–12*), reasonably complete skeletons have been recovered only from South America (*13*), where abelisaurid predators and titanosaurian herbivores flourished.

On continental Africa, the most complete remains of Late Cretaceous dinosaurs were discovered in Egypt and include the lower jaw and vertebrae of an unusual finbacked theropod, *Spinosaurus* (*3*); skull fragments and bones of another large theropod, *Carcharodontosaurus* (*4*); isolated bones of a third predator, *Bahariasaurus* (*5*); and bones of a large titanosaurian sauropod, *Aegyptosaurus* (*6*). In beds of similar age in Morocco, several bones of an enigmatic sauropod *Rebbachisaurus* were discovered (*7*). Phylogenetic interpretation of these remains (*14–17*) has been difficult because many of the bones are fragmentary and because the Egyptian collection was destroyed during World War II (*18*).

We describe here new vertebrate remains from Late Cretaceous beds in the

P. C. Sereno, H. C. E. Larsson, P. M. Magwene, C. A. Sidor, J. A. Wilson, Department of Organismal Biology and Anatomy, University of Chicago, 1027 East 57th Street, Chicago, IL 60637, USA.
D. B. Dutheil, 48 rue de la Rochefoucauld, 75009 Paris, France.
M. Iarochene, Ministère de l'Energie et des Mines, Rabat, Morocco.
G. H. Lyon, 3551 Carter Hill Road, Montgomery, AL 36111, USA.
D. J. Varricchio, Old Trail Museum, Post Office Box 919, Choteau, MT 59422, USA.

*To whom correspondence should be addressed. Co-authors are listed alphabetically.

Kem Kem region of southeastern Morocco (Fig. 1, A and B). The fossiliferous horizons are exposed along the face of an escarpment formed by a carbonate platform of Late Cenomanian through Turonian age (*19*). The beds beneath the platform have been divided informally into a lower red sandstone unit (*grés rouges infracénomaniens*) and an upper marly unit (*marne versicolores à gypse*) (*20*). This general description, however, only characterizes the underlying beds in the Kem Kem region (*21*).

We informally recognize this distinct, nonmarine deltaic facies as the Kem Kem beds, which can be divided equally into two units that together attain a maximum thickness of approximately 200 m (Fig. 1C) (*22*). Nonvertebrate and vertebrate remains have been recovered, the latter preserved largely as disarticulated elements (*23*). Nine elasmobranch species strongly support a Cenomanian age for the deposit [circa (ca.) 93 million years ago (Ma)] (*24*). Dinosaurs are represented by several theropods, at least two sauropods, and a large iguanodontian (*25*).

These fossils include a relatively complete theropod skull lacking the lower jaws (Fig. 2, A and B) (*26*) and a partial skeleton of a second theropod (Fig. 3). Approximately 1.6 m in length, the skull equals or exceeds the length of the largest known skull of *Tyrannosaurus rex* (*27*). The maxilla has sockets for 14 blade-shaped teeth, the crowns of which are diagnostic in shape and ornamentation (Fig. 2C). The posterior margin of the crown is only slightly recurved and becomes convex toward the crown tip. On both sides of the crown, arcuate enamel wrinkles curve toward the marginal serrations and often extend across the crown as low bands (Fig. 2C). These dental features allow reference of the skull to *Carcharodontosaurus saharicus* (*28*), a species based originally on isolated teeth from western Algeria (*7*) and later represented by cranial fragments and postcranial bones from Egypt (*4*, *5*) and teeth from Niger (*9*), Tunisia (*10*), and Sudan (*11*).

The cranium tapers anteriorly in side view and is narrow in dorsal view (Fig. 2, A and B). The antorbital fenestra is exceptionally large (30% of skull length), and pneumatic extensions of the antorbital fossa open into the surrounding bones (maxilla, nasal, lacrimal, and jugal). The protruding ventral margin of the fossa, the sculptured surface of the maxilla, and the rugose nasals also characterize the Egyptian cranial elements, which are associated with postcranial bones (*4*, *29*). The stout, strongly opisthocoelous cervical vertebrae of *C. saharicus* are diagnostic and have low neural spines, robust transverse processes, and exceptionally broad, keeled centra (Fig. 2D).

Cladistic analysis of basal tetanurans places *Carcharodontosaurus* within the allosauroid clade (Fig. 4A) as recently suggested (*17*), allying it closely with *Acrocanthosaurus* from the Albian of North America (*30*) and *Giganotosaurus* from the Albian or Cenomanian of South America (*31*). Characters that unite these taxa as carcharodontosaurids include a broad orbital shelf (formed by the lacrimal and postorbital bones) and the squared anterior end of the lower jaw. In *Carcharodontosaurus* and *Acrocanthosaurus*, the cervical centra are particularly broad, and the anterior caudal vertebrae have small pleurocoels.

The new fossils also include a partial skeleton, several bones of which (the coracoid, femur, and fibula) are identical to bones referred to the Egyptian species *Bahariasaurus ingens* (*5*). These Egyptian bones, however, are not part of the holotypic specimen of *B. ingens*, which is based on other fragmentary postcranial elements (*32*). Therefore, we designate the Moroccan skeleton as the holotype of a new theropod, *Deltadromeus agilis*, gen. nov., sp. nov., to which we refer several of the Egyptian bones (*33*).

The limb bones in *Deltadromeus* are remarkably slender. Length/diameter ratios are similar to those in the smaller cursorial coelurosaur *Ornithomimus* and are only 50 to 60% of the diameter of those in the equal-sized allosauroid *Allosaurus* (Table 1). The plate-shaped coracoid and proximal scapula in *Deltadromeus* are broader than in other theropods that also show expansion of the acromial region (therizinosaurids, tyrannosaurids, and deinonychosaurs). On the basis of the preserved portions of the humerus, radius, and ulna, the forelimb is not substantially reduced in length. The cursorial proportions of the hind limb bones lie between those for *Allosaurus* and *Ornithomimus* (Table 1).

The phylogenetic analysis suggests that *Deltadromeus* is an early derivative of the coelurosaur radiation (Fig. 4A) and most closely resembles the smaller Late Jurassic taxon *Ornitholestes* (*34*). Its status as a

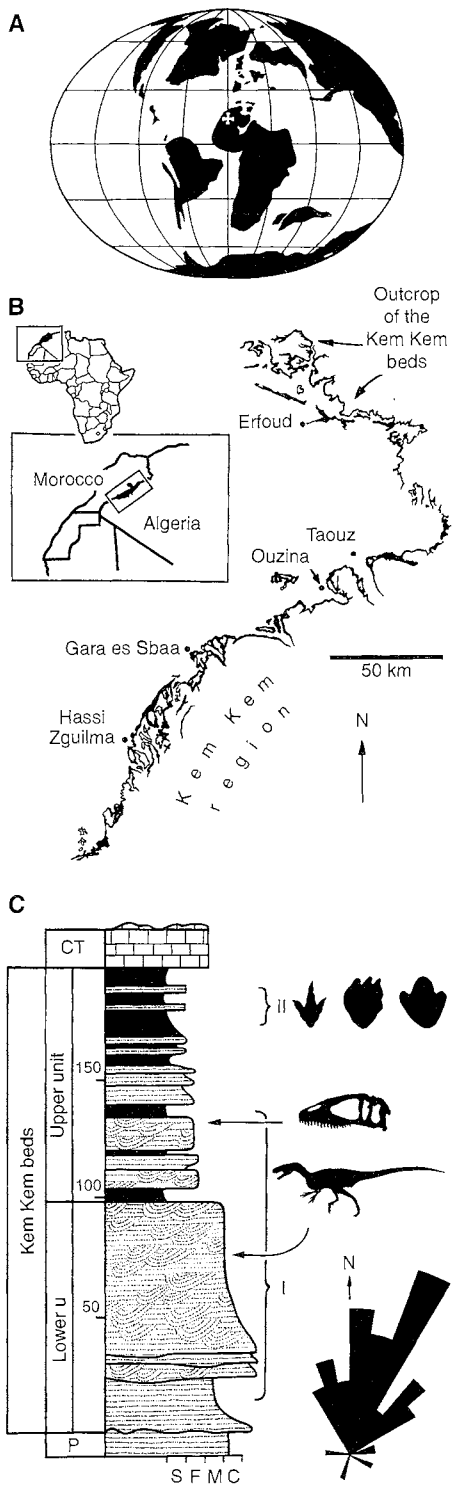

Fig. 1. Late Cretaceous paleogeography and principal exposures of the Kem Kem beds. (**A**) Late Cretaceous (Cenomanian, 90 to 97 Ma) paleogeographic map (Mollweide projection) with latitude and longitude lines spaced at 30° intervals (longitude greater than 120° not shown) (*41*). White cross indicates fossil locality. (**B**) Maps showing Morocco and the location of ribbon-shaped exposures of the Kem Kem beds in southeastern Morocco. (**C**) Section of the Kem Kem beds at Gara es Sbaa showing the erosional contact below with Ordovician and Devonian strata and a conformable contact above with the Cenomanian-Turonian limestone platform (brick pattern). Sandstone (stipple) dominates the lower unit, whereas mudstone (solid) increases within the upper unit. Measurements are in meters. Silhouettes show the principal kinds of footprints in the footprint zone (upper right) and the stratigraphic level of the skull of *Carcharodontosaurus* and skeleton of *Deltadromeus* (middle right). Paleocurrent rose diagram (lower right) shows strong northerly orientation of cross-stratification within the lower unit of the Kem Kem beds (n = 43; mean = N15°E). CT, Cenomanian-Turonian; P, Paleozoic; S F M C, silt, fine-, medium-, and coarse-grained sandstone; I, fossiliferous zone; II, footprint zone.

coelurosaur is based on the expansion of the coracoid, the reduction of the femoral fourth trochanter to a low ridge, and the presence of a large deep fossa on the proximal end of the fibula (Fig. 3, E, G, and H).

Late Cretaceous fossils from Africa are critical for the establishment of biogeographic patterns toward the end of the Mesozoic. During this time, an endemic fauna had arisen in Asiamerica (central Asia and western North America) that consisted almost entirely of coelurosaurian predators and ornithischian herbivores (*1*). A complementary Gondwanan dinosaurian fauna composed of abelisaurid and spinosaurid predators and titanosaurian sauropods has been described (*35*) but has yet to be clearly established on, and restricted to, southern continents other than South America (*15*, *36*).

The dinosaur remains from Morocco support the following biogeographic conclusions:

1) During the Late Cretaceous, several large theropods achieved a trans-African distribution. The Moroccan material indicates that at least three large predators (*Spinosaurus*, *Carcharodontosaurus*, and *Deltadromeus*) ranged across north Africa during the Late Cretaceous (Cenomanian).

2) During the Early Cretaceous, large carcharodontosaurid predators underwent a global radiation. The close relations between *Carcharodontosaurus* (African), *Acrocanthosaurus* (North American), and *Giganotosaurus* (South American) identify a carcharodontosaurid radiation that had achieved a transcontinental distribution before the end of the Early Cretaceous (ca. 100 Ma) (Fig. 4B). *Carcharodontosaurus* may have been isolated on Africa during the Cenomanian (ca. 90 Ma), as paleogeographic reconstructions suggest, but its carcharodontosaurid progenitors were able to colonize northern and southern landmasses during the Early Cretaceous.

3) By the Late Jurassic, basal coelurosaurs had achieved a global distribution. *Deltadromeus* and recent discoveries of maniraptoran bones in Sudan and Argentina (*37*) document the presence of coelurosaurs on southern continents during the Late Cretaceous. The early divergence of a lineage that gave rise to *Deltadromeus* suggests that primitive coelurosaurs were present on southern continents before the close of the Jurassic.

4) At the beginning of the Late Cretaceous (Cenomanian), a distinctive dinosaurian fauna was present in Africa. Thus far, only Africa has yielded Late Cretaceous spinosaurids, primitive coelurosaurs like *Deltadromeus*, abundant small theropods with simple blade-shaped teeth, and a large iguanodontoid (*25*). Although the sauropod *Rebbachisaurus* may share its closest relations with a South American form (*38*), the Moroccan dinosaurian fauna is distinct from Cenomanian faunas on South America and northern continental areas, where abelisaurids and titanosaurs (South America) and hadrosaurs, ankylosaurs, and deinonychosaurs (northern continents) are dominant (*39*). It

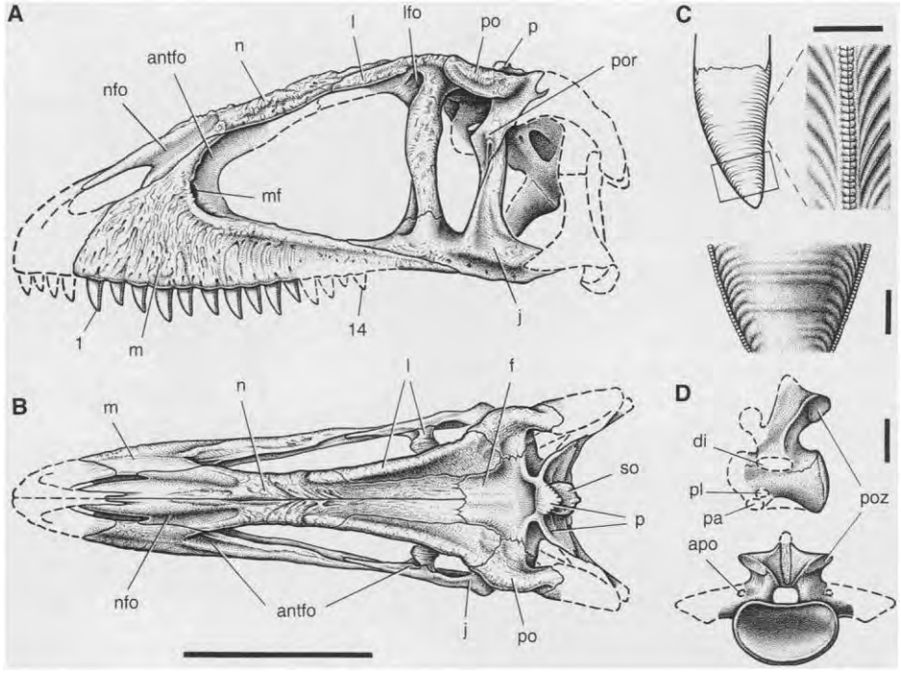

Fig. 2. Cranium and maxillary tooth (SGM-Din 1) and postaxial cervical vertebra (SGM-Din 3) of *C. saharicus*. Cranial reconstruction is shown in (**A**) left lateral and (**B**) dorsal views. Stippling indicates bone preserved on at least one side of the cranium. (**C**) Maxillary tooth from cranium in left lateral view, with magnified views of the posterior margin (right) and lateral surface (below). (**D**) Midcervical vertebra in (top) left lateral and (bottom) posterior views. Scale bar in (A) and (B), 50 cm; in (C), 5 mm (above) and 1 cm (below); in (D), 5 cm. Abbreviations: antfo, antorbital fossa; apo, accessory pneumatic opening; di, diapophysis; f, frontal; j, jugal; l, lacrimal; lfo, lacrimal fossa; m, maxilla; mf, maxillary fenestra; n, nasal; nfo, narial fossa; p, parietal; pa, parapophysis; pl, pleurocoel; po, postorbital; por, postorbital rugosity; poz, postzygapophysis; and so, supraoccipital.

Table 1. Length and minimum diameter measurements (in millimeters) and ratios in *D. agilis* (SGM-Din 2), *Allosaurus fragilis* (*44*), and *Ornithomimus* sp. (Royal Tyrrell Museum of Palaeontology, Drumheller, Alberta, Canada, uncataloged). Parentheses indicate estimation; dashes indicate missing information.

Bone	*Deltadromeus*	*Allosaurus*	*Ornithomimus*
	Length, diameter		
Midcaudal centrum	130, 70	—	—
Distal caudal centrum	130, 35	90, 28	—
Humerus	(328), 22	310, 38	—
Femur	740, 53	850, 95	418, (46)
Tibia	(700), —	690, 72	485, (35)
Metatarsal II	417, 20	270, 42	300, 25
Metatarsal III	450, 22	327, 40	332, (16)
Metatarsal IV	400, 20	275, 36	311, 25
Metatarsal V	100, 8	—	120, 7
Digit II–phalanx 1	140	120	68
Digit II–ungual	80	80	52
Digit III–phalanx 1	140	110	—
Digit IV–phalanx 1	98	75	40
Digit IV–phalanx 1	98	75	40
Digit IV–phalanx 3	52	30	22
Digit IV–phalanx 4	37	29	21
	Ratios		
Humerus/femur	(0.44)	0.36	—
Tibia/femur	(0.95)	0.73	1.16
Metatarsal III/femur	0.61	0.52	0.79
Metatarsal III/tibia	(0.64)	0.47	0.69

remains to be determined whetherAfrica's Cenomanian dinosaurian fauna persisted to the end of the Cretaceous.

5) The Moroccan fossils suggest, in conclusion, that substantial faunal exchange between major land areas may have continued well into the Early Cretaceous. Marked provincialism of dinosaurian faunas in North America, South America, and Africa appears to have abruptly arisen early in the Late Cretaceous, when dispersal routes between northern and southern

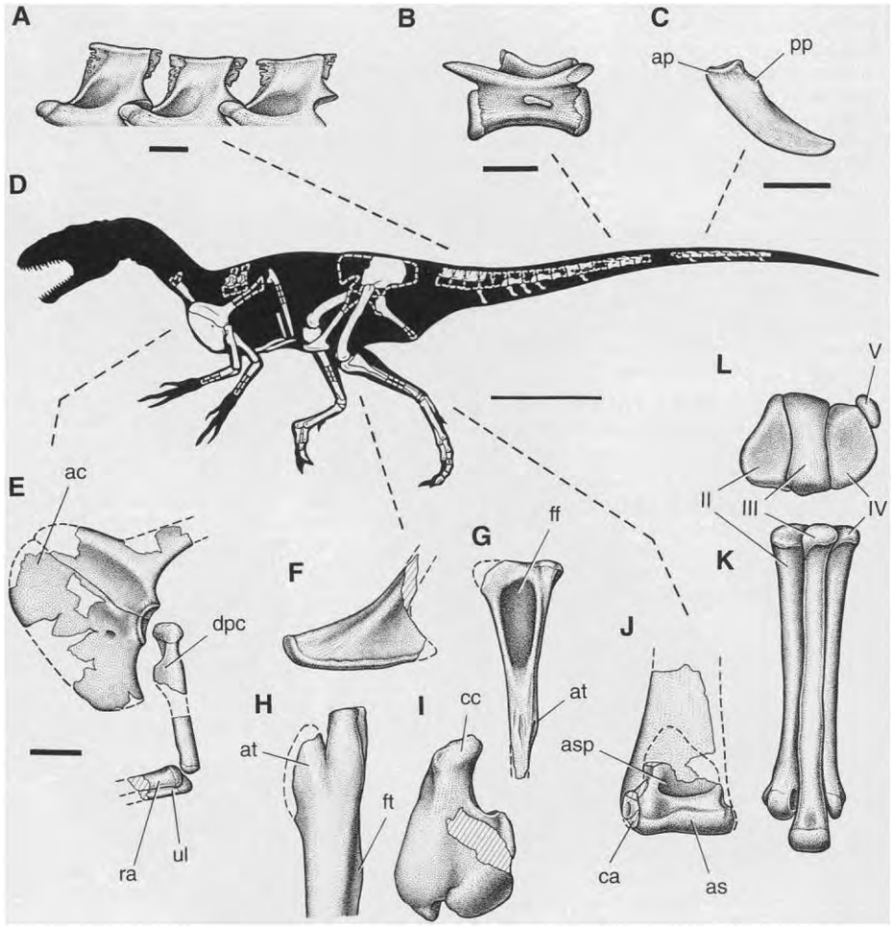

Fig. 3. Skeletal anatomy of *D. agilis* (SGM-Din 2). (**A**) Neural spines of anterior caudal vertebrae in left lateral view. (**B**) Midcaudal vertebra in left lateral view. (**C**) Midcaudal chevron in left lateral view. (**D**) Skeletal reconstruction showing preserved bones (length of *D. agilis* approximately 9 m). (**E**) Scapulocoracoid and forelimb (composite left and right) in left lateral view. (**F**) Pubic foot in left lateral view. (**G**) Proximal left fibula in medial view. (**H**) Proximal femur (reversed from right) in left lateral view. (**I**) Tibia (reversed from right) in proximal view (anterior toward top). (**J**) Distal tibia, astragalus, and calcaneum (reversed from right) in anterior view. (**K**) Left metatarsals II to IV in anterior view. (**L**) Left metatarsals II to V in proximal view (anterior toward bottom). Scale bar in (A), 5 cm [also for (F), (G), (H), and (K)]; in (B), 5 cm [also for (I), (J), and (L)]; in (D), 1 m; in (E), 10 cm. Abbreviations: ac, acromion; ap, anterior process; as, astragalus; asp, ascending process; at, anterior trochanter; ca, calcaneum; cc, cnemial crest; dpc, deltopectoral crest; ff, fibular fossa; ft, fourth trochanter; pp, posterior process; ra, radius; and ul, ulna.

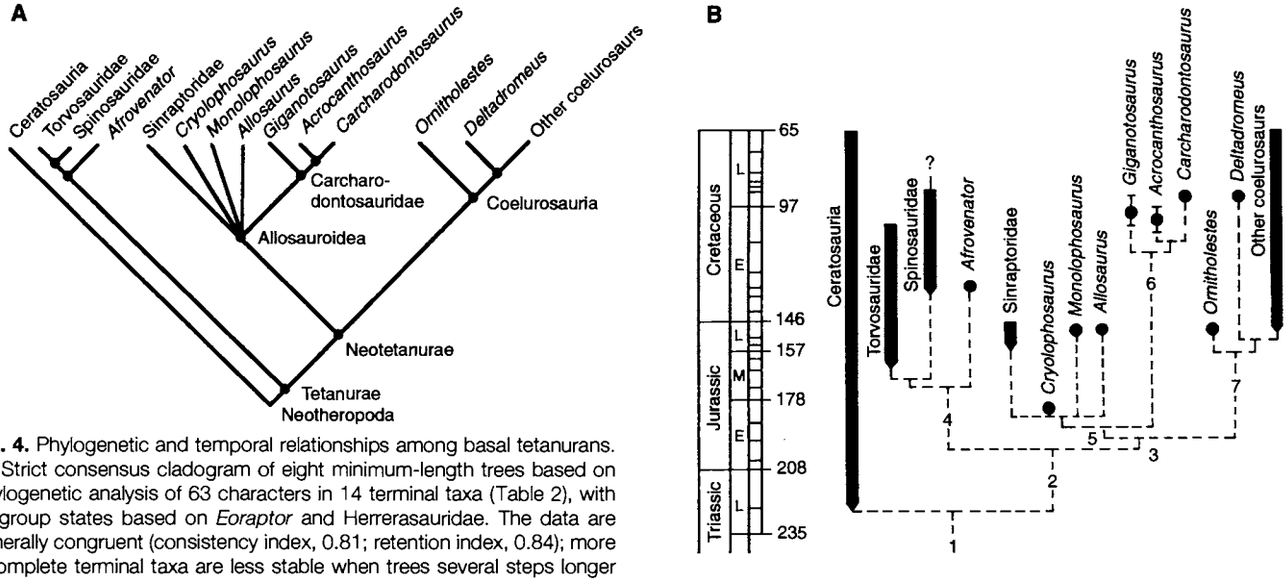

Fig. 4. Phylogenetic and temporal relationships among basal tetanurans. (**A**) Strict consensus cladogram of eight minimum-length trees based on phylogenetic analysis of 63 characters in 14 terminal taxa (Table 2), with outgroup states based on *Eoraptor* and Herrerasauridae. The data are generally congruent (consistency index, 0.81; retention index, 0.84); more incomplete terminal taxa are less stable when trees several steps longer than the minimum are sampled (*42*). (**B**) Phylogram based on the cladogram and recorded temporal ranges as calibrated on a recent time scale (*43*). Error bars indicate age uncertainty. 1, Neotheropoda; 2, Tetanurae; 3, Neotetanurae; 4, Spinosauroidea; 5, Allosauroidea; 6, Carcharodontosauridae; 7, Coelurosauria.

Table 2. Character state matrix for an outgroup (based on *Eoraptor* and Herrerasauridae), 14 ingroups, and 63 characters (*45*) used in a phylogenetic analysis of basal tetanurans (Fig. 4) (*42*).

Taxa	Characters												
	10			20		30		40		50		60	
Outgroup	00000	00000	00000	00000	0?000	00?00	00000	00000	00000	00000	00000	00000	000
Ceratosauria	10000	00000	00000	00000	0?000	00000	00000	0000?	00000	00000	00000	00000	000
Afrovenator	11111	11111	11111	11111	10???	0??00	?0111	1?0??	00???	0?000	0?000	0?0?0	?00
Torvosauridae	011?1	??1??	10?11	11111	10???	0?000	?1111	111?0	?0?0?	0?00?	00000	0?000	0?0
Spinosauridae	????1	?????	11???	?????	?????	??1??	?11??	?11??	?????	?00?0	?101?	0??0?	???
Sinraptoridae	11111	11??1	11111	11111	11111	??011	10000	0??11	11111	00000	00000	00000	000
Cryolophosaurus	?1???	1????	???01	?????	????1	?????	??0?0	????1	1??11	01000	?0?0?	0????	?0?
Monolophosaurus	11?1?	11???	11???	?????	?1?1?	????1	?1??0	0??1?	1??1?	11000	00000	0?0?0	0??
Allosaurus	1111?	11111	11111	11111	11111	11111	10000	00011	11111	11000	10000	000?0	100
Giganotosaurus	11???	?????	111??	1???1	?1???	??111	?0000	0???1	?0???	0?111	1?0??	0?000	10?
Acrocanthosaurus	1111?	11?11	?1111	11??1	111?1	??1??	?00?0	?0?11	0??0?	01111	11111	00000	??0
Carcharodontosaurus	1111?	1?1??	???1?	?????	?1???	?????	?0000	???11	0??0?	??11?	?1111	0?0??	?00
Ornitholestes	1111?	1?1?1	111?1	????1	11111	1??11	?0000	0000?	0?0?0	00000	00000	111?1	110
Deltadromeus	?????	??1??	??111	11111	1????	1?1??	?????	?????	0????	?????	?????	???1?	?11
Other coelurosaurs	111?1	1111	1111	21102	1111	11111	10000	00000	00000	01000	10000	11111	111

land areas were finally severed and when oceanic barriers had arisen between southern continents.

REFERENCES AND NOTES

1. Coelurosaurs include ornithomimids, tyrannosaurids, and maniraptorans. Ornithischians include ankylosaurs, hadrosaurids, pachycephalosaurs, and ceratopsians.
2. **Antarctica**: E. B. Olivero *et al.*, in *Geological Evolution of Antarctica*, M. R. A. Thomson, J. A. Crame, J. W. Thomson, Eds. (Cambridge Univ. Press, Cambridge, 1987), pp. 617–622; Z. Gasparini *et al.*, *Anais do X Congresso Brasileiro de Paleontologia*, Rio de Janeiro, Brazil, 19 to 25 July 1987, pp. 131–139. J. J. Hooker, A. C. Milner, S. E. K. Sequeira, *Antarct. Sci.* **3**, 331 (1991). **Australia**: R. E. Molnar, *Mem. Soc. Geol. Fr.* **139**, 131 (1980); W. P. Coombs and R. E. Molnar, *Mem. Queensl. Mus.* **20**, 351 (1981). **India**: F. von Huene and C. A. Matley, *Mem. Geol. Surv. India* **21**, 1 (1933); S. Chatterjee, *J. Paleontol.* **52**, 570 (1978); D. S. Berman and S. L. Jain, *Ann. Carnegie Mus.* **51**, 405 (1982). **Madagascar**: C. Depéret, *Bull. Soc. Geol. Fr.* **24**, 176 (1896); R. Lavocat, *Mus. Natl. Hist. Nat.* **27**, 256 (1955).
3. E. Stromer, *Abh. Kgl. Akad. Wiss. Math. Phys. Kl.* **28**, 1 (1915).
4. ———, *Abh. Bayer. Akad. Wiss. Math. Naturwiss. Abt. N. F.* **9**, 1 (1931).
5. ———, *ibid.* **22**, 1 (1934).
6. ———, *ibid.* **9**, 1 (1932).
7. C. Depéret and J. Savornin, *C. R. Acad. Sci. Paris* **181**, 1108 (1925); *Bull. Soc. Geol. Fr.* **27**, 257 (1927).
8. R. Lavocat, *C. R. Acad. Sci. Paris* **232**, 169 (1951); *Comptes rendus 19e Congrès géologique international (Alger.) 1952* (Academie des Sciences de Paris, Paris, 1954), pp. 65–68.
9. A. F. de Lapparent, *Mem. Soc. Geol. Fr.* **88A**, 1 (1960).
10. ———, *C. R. Acad. Sci. Paris* **232**, 1430 (1951); S. Bouaziz *et al.*, *Bull. Soc. Geol. Fr.* **1988**, 335 (1988).
11. C. Werner, *Berl. Geowiss. Abh.* **13**, 221 (1994).
12. E. Stromer, *Abh. Bayer. Akad. Wiss. Math. Naturwiss. Abt. N. F.* **10**, 1 (1932); F. de Broin *et al.*, *C. R. Acad. Sci. Paris* **279**, 469 (1974); W. J. Kennedy, H. C. Klinger, N. J. Mateer, *S. Afr. J. Sci.* **83**, 173 (1987); E. Buffetaut, *Neues Jahrb. Geol. Palaeontol. Monatsh.* **1989**, 79 (1989).
13. F. von Huene, *An. Mus. La Plata* (ser. 2) **3**, 1 (1929); J. F. Bonaparte and J. E. Powell, *Mem. Soc. Geol. Fr.* **139**, 19 (1980); J. F. Bonaparte and F. E. Novas, *Ameghiniana* **21**, 259 (1985); J. E. Powell, *Mus. Argent. Cienc. Nat. Paleontol.* **3**, 147 (1987); J. F. Bonaparte, F. E. Novas, R. A. Coria, *Nat. Hist. Mus. Los Angel. Cty. Contrib. Sci.* **416**, 1 (1990); J. E. Powell, in *Los Dinosaurios y Su Entorno Biotico*, J. L. Sanz and A. D. Buscalioni, Eds. (Instituto Juan de Valdes, Cuenca, Spain, 1992), pp. 165–230.
14. The phylogenetic position of *Spinosaurus* among basal tetanurans (*15*) (Fig. 4) is based largely on more complete spinosaurid remains discovered recently in the Lower Cretaceous of England [A. J. Charig and A. C. Milner, in *Dinosaur Systematics: Perspectives and Approaches*, K. Carpenter and P. J. Currie, Eds. (Cambridge Univ. Press, Cambridge, 1990), pp. 127–140].
15. P. C. Sereno *et al.*, *Science* **266**, 267 (1994).
16. R. E. Molnar, S. M. Kurzanov, Z. Dong, in *The Dinosauria*, D. B. Weishampel, P. Dodson, H. Osmólska, Eds. (Univ. of California Press, Berkeley, CA, 1990), pp. 169–209; J. McIntosh, *ibid.*, pp. 345–401.
17. O. W. M. Rauhut, *Berl. Geowiss. Abh.* **16**, 357 (1995).
18. The fossils were destroyed during a bombing raid on Munich in 1944 by the British Royal Air Force {U.S. forces were not involved, contrary to E. Buffetaut and G. Cuny [*Science* **267**, 1751 (1995)]}.
19. The well-dated platform [M. Ferrandini *et al.*, *Bull. Soc. Geol. Fr.* **1**, 559 (1985)] marks the onset of a major transgression in the Late Cenomanian that inundated all of northern Africa [C. Meister *et al.*, *Geobios* **25**, 55 (1991); J. Hardenbol *et al.*, *Cretaceous Res.* **14**, 449 (1993)].
20. G. Choubert, *Notes Mem. Serv. Geol. Maroc* **100**, 75 (1952). These beds are commonly cited as "*continentale intercalaire*" or "*infra-Cénomanien*" [A. F. de Lapparent, *J. Paleontol. Soc. India* **2**, 109 (1957); R. Lavocat, *Notes Mem. Serv. Geol. Maroc* **116**, 1 (1954); N. J. Mateer *et al.*, *Cretaceous Res.* **13**, 273 (1992)] and recently have been attributed incorrectly to the Tegana Formation [D. B. Weishampel, in *The Dinosauria*, D. B. Weishampel, P. Dodson, H. Osmólska, Eds. (Univ. of California Press, Berkeley, CA, 1990), p. 109].
21. The underlying beds west of Goulmima [H. Gauthier, *Notes Mem. Serv. Geol. Maroc* **119**, 1 (1957)] and north of Anoual (our section data), in contrast, consist of a marginal marine-evaporite facies characterized by alternating marl, limestone, and gypsum that do not compose two distinct, subequal subunits.
22. The Kem Kem beds, which thin to about 100 m toward the south (near Hassi Zguilma) and east (near Taouz), are a nonmarine deltaic facies, as shown by included fossils (decapods, shrimp, and diverse shark teeth), sedimentary structures (mud drapes and flaser bedding), and consistent north-trending paleocurrents toward contemporaneous marginal marine facies (Fig. 1C). Footprint horizons and other subaerial trace fossils occur within 7 m of the Cenomanian-Turonian platform, suggesting that the overlying marine transgression was abrupt. The **lower unit** is composed almost exclusively of reddish, fine- to coarse-grained, planar and trough cross-stratified sandstone, with lateral accretion deposits. Pebble channels, vertical burrows, and rolled vertebrate fossils (bone, scales, and teeth) are common above the basal 15 m; and soft sediment deformation, mudstone lenses, and primary or secondary gypsum are rare. The **upper unit** fines upward and is composed of red to tan, coarse- to fine-grained sandstones intercalated with variegated mudstones in roughly equal amounts. Bioturbation, ripple marks, mud cracks, footprint horizons, and soil slickensides are locally abundant, gypsum is rare or absent, and the sandstones alone are fossiliferous.
23. Common nondinosaurian vertebrates in the fauna include small notosuchid crocodilians, at least one large crocodilian (cf. *Sarcosuchus*), varanid lizards, a palaeophid snake, a dipnoan (cf. *Ceratodus*), a coelacanth (cf. *Mawsonia*), bony fishes (polypterids, lepisosteids, amiids, and pycnodonts), and elasmobranchs.
24. Seven of the nine elasmobranchs in the Kem Kem beds also occur in the Cenomanian Bahariya Formation [B. H. Slaughter and J. T. Thurmond, *Ann. Geol. Surv. Egypt* **4**, 25 (1974); W. Dominik, *Berl. Geowiss. Abh.* **A62**, 173 (1985); C. Werner, *Palaeoichthyologica* **5**, 1 (1989)], including four species limited to these formations (*Distobatus nutiae*, "*Lissodus*" *bartheli*, *Marckgrafia libyca*, and *Peyeria libyca*), and one species with a broad distribution that is restricted to the Cenomanian [*Serratolamna amonensis*; H. Cappetta and G. R. Case, *Geobios* **8**, 303 (1975)].
25. Sauropod remains include vertebrae of *Rebbachisaurus garasbae* and narrow-crowned titanosaur teeth with high-angle wear facets. A large ornithopod is known from a clover-leaf–shaped footprint measuring approximately 50 cm in length and width (Fig. 1C) [T. Thulborn, *Dinosaur Tracks* (Chapman and Hall, London, 1990), pp. 190–191]. *Spinosaurus* cf. *S. aegyptiacus* is represented by jaw fragments and teeth, and small theropods are known from teeth and a pair of fused nasals with a median crest. Other disarticulated dinosaurian remains have been reported recently from the Kem Kem beds [D. A. Russell, *Bull. Mus. Nat. Hist. Nat.* (Paris), in press].
26. The skull (SGM-Din 1) is in the collections of the Ministère de l'Energie et des Mines, Rabat, Morocco.
27. *C. saharicus*, *Giganotosaurus carolinii* (*31*), and *T. rex* grew to similar adult sizes. The reconstructed cranium of *C. saharicus* (SGM-Din 1) has a length of about 160 cm (measured as a straight line from the anterior end of the premaxilla to the posterior margin of the quadrate) and is about 15% larger than the Egyptian specimen (*4*). The largest cranium of *T. rex* is somewhat shorter (153 cm; South Dakota specimen), with average skull length about 15% shorter (*40*). Skull size in *G. carolinii* is similar to that of *C. saharicus* (SGM-Din 1) where they overlap. Available limb bone lengths for *C. saharicus* are limited to the femur and fibula of the smaller Egyptian specimen (*4*), which (scaled up 15%) yields a femoral length estimate of 145 cm for SGM-Din 1. Combined femoral and tibial lengths in *G. carolinii* (143 cm and 112 cm; total, 255 cm) are approximately equal to those

for the largest tyrannosaur (138 cm and 120 cm; total, 258 cm). Skull length may thus be proportionately greater in carcharodontosaurids than in tyrannosaurids, which appear to have longer distal hind limbs segments.
28. Diagnostic features for *C. saharicus*. **Dental:** Posterior crown margin only slightly concave at mid-length and convex distally; enamel ornamentation, including transverse bands and arcuate wrinkles near crown margins. **Cranial:** Antorbital fenestra length 30%, and height 25%, of those of the cranium; ventral margin of antorbital fossa everted; prefrontal absent or co-ossified; postorbital ventral ramus with robust lateral process with groove and pit; postorbital-squamosal articulation helical; and paroccipital processes and basal tubera positioned far ventral to occipital condyle. **Postcranial:** Postaxial cervical vertebrae with kidney-shaped posterior articular faces, short neural spines, robust transverse processes, and strong ventral keels; anterior caudal vertebrae with pleurocoels; and distal caudal vertebrae with narrow anteroposteriorly compressed neural spines.
29. Stromer's skeleton 1922 X46 provides an association between cranial and postcranial bones, including an exceptionally broad cervical vertebra and a pleurocoelous anterior caudal vertebra (*4*). These vertebrae, in turn, overlap with skeleton 1922 X45 (Stromer's "*Spinosaurus* B"), which provides additional information about the vertebral column and pedal phalanges (*5*).
30. J. W. Stovall and W. Langston Jr., *Am. Midl. Nat.* **43**, 696 (1950).
31. R. A. Coria and L. Salgado, *Nature* **377**, 224 (1995).
32. The holotypic specimen of *B. ingens* comprises two dorsal vertebrae, a neural arch, three sacral vertebrae, a rib fragment, pubes, and the proximal portion of the ischium (1922 X47) (*5*). Unlike the Moroccan skeleton, the shaft of the pubis is broader, the pubic foot is divided in the midline, and the iliac peduncle of the ischium is proportionately narrower.
33. **Etymology:** *Delta*, delta (Greek); *dromeus*, runner (Greek); *agilis*, quick (Latin). Named for the deltaic facies in which it was found and for the cursorial proportions of its hind limbs. The holotypic skeleton (SGM-Din 2) is in the collections of the Ministère de l'Energie et des Mines, Rabat, Morocco. **Diagnosis:** Anterior caudal vertebrae with broad quadrangular neural spines; coracoid and acromion broadly expanded anteroposteriorly; coracoid with shallow notch in anterior margin; ischial midshaft dorsoventrally compressed; femur with accessory trochanter on distal shaft; femoral medial distal condyle with anterior extension; metatarsal IV distal condyles reduced. **Referred material** (existing as figures only): Left coracoid, pubes, right femur, proximal right tibia, and left fibula (1912 VIII) (*5*). Femoral length (122 cm) is 1.5 times that of SGM-Din 2, indicating that *D. agilis* grew to an adult body size within the range established for *T. rex* (*40*).
34. H. F. Osborn, *Bull. Am. Mus. Nat. Hist.* **35**, 733 (1916).
35. J. F. Bonaparte and Z. Kielan-Jaworowska in *Fourth Symposium on Mesozoic Terrestrial Ecosystems, Short Papers*, P. J. Currie and E. H. Koster, Eds. (Occasional Paper 3, Royal Tyrrell Museum of Palaeontology, Drumheller, Alberta, Canada, 1987), pp. 24–29.
36. R. Molnar, *Mem. Soc. Geol. Fr.* **139**, 131 (1980); E. Buffetaut and J.-C. Rage, in *The Africa–South America Connection*, W. George and R. Lavocat, Eds. (Clarendon, Oxford, 1993), pp. 87–99.
37. J. F. Bonaparte, *Mus. Argent. Cienc. Nat. Paleontol.* 4, 16 (1991); O. W. M. Rauhut and C. Werner, *Palaeontol. Z.* **69**, 475 (1995).
38. J. Calvo and L. Salgado, *Gaia*, in press.
39. J. I. Kirkland and D. Burge, *J. Vertebr. Paleontol.* **14**, 32A (1994).
40. P. L. Larson, *Paleontol. Soc. Spec. Pub.* **7**, 139 (1995).
41. A. G. Smith, D. G. Smith, B. M. Funnell, *Atlas of Mesozoic and Cenozoic Coastlines* (Cambridge Univ. Press, Cambridge, 1994), p. 38.
42. D. L. Swofford, PAUP 3.1 (Illinois Natural History Survey, Champaign, IL, 1993).
43. W. B. Harland *et al.*, *A Geologic Time Scale 1989* (Cambridge Univ. Press, Cambridge, 1990).
44. C. W. Gilmore, *Bull. U.S. Nat. Mus.* **110**, 1 (1920).
45. The following 63 synapomorphies correspond with scored character states (Table 2) that were used in the analysis of basal tetanuran relationships presented in Fig. 4. **Tetanurae: 1**, maxillary fenestra; **2**, lacrimal pneumatic excavation; **3**, slot in ventral process of lacrimal for jugal; **4**, jugal pneumatic excavation; **5**, prefrontal-frontal peg-in-socket articulation; **6**, posteriormost maxillary tooth positioned anterior to orbit; **7**, axial neural spine broadened distally; **8**, chevron bases with paired anterior and posterior processes; **9**, semilunate carpal with transverse trochlea; **10**, manual digit III reduced (metacarpal III shaft diameter is 50% or less that of metacarpal II); **11**, iliac-ischial articulation smaller than iliac-pubic articulation; **12**, ischial obturator notch; **13**, femoral anterior trochanter blade-shaped; **14**, tibial distal end backing calcaneum; **15**, fibular distal end reduced (less than twice anteroposterior width at midshaft); **16**, astragalar ascending process plate-shaped (state 1); **17**, astragalar cup for fibula reduced; **18**, astragalar distal condyles oriented anteroventrally; **19**, astragalar condyle with anterior groove; **20**, metatarsal III with hourglass-shaped proximal end; **21**, metatarsal III with wedge-shaped midshaft. **Neotetanurae: 22**, promaxillary recess extends into maxillary anterior ramus; **23**, ectopterygoid pneumatic excavation invaginated laterally; **24**, splenial with notched anterior margin of internal mandibular fenestra; **25**, retroarticular surface of articular facing posteriorly; **26**, posterior chevrons L-shaped; **27**, furcula (fused clavicles); **28**, coracoid posterior process and fossa crescent-shaped; **29**, iliac preacetabular fossa present; **30**, iliac pubic peduncle twice as long anteroposteriorly as broad transversely; **31**, pedal digit I–phalanges 1 + 2 subequal in length to pedal digit III–phalanx 1. **Spinosauroidea** (plus included node): **32**, anterior ramus of maxilla as long anteroposteriorly as tall; **33**, lacrimal anterior ramus dorsoventrally narrow; **34**, lacrimal foramen small, positioned at mid-height along ventral ramus; **35**, postorbital ventral process with U-shaped cross section; **36**, quadrate foramen reduced or absent; **37**, radius less than 50% of humeral length; **38**, manual digit I ungual elongate (three times the height of proximal articular end). **Allosauroidea** (plus unresolved subgroups): **39**, nasal participation in antorbital fossa; **40**, excavated internal carotid artery canal; **41**, basipterygoid processes very short; **42**, quadrate with broad articular flange for quadratojugal; **43**, palatine with flange-shaped process for lacrimal; **44**, basioccipital excluded from the basal tubera; **45**, articular with pendant medial process; **46**, quadrate short, head near mid-orbit; **47**, surangular twice maximum depth of angular (which equals a reduced external mandibular fenestra). **Carcharodontosauridae** (plus included node): **48**, broad postorbital-lacrimal contact; **49**, postorbital with suborbital flange; **50**, dentary with squared, expanded anterior end; **51**, pubic boot 30% of pubic length; **52**, ventral extension of basisphenoid; **53**, midcervical centra (posterior articular face) at least 20% broader than tall; **54**, elevation of anterior face absent in midcervical centra; **55**, rudimentary caudal pleurocoels. **Coelurosauria** (plus included node): **56**, antorbital fossa anterior margin 40 to 50% of the anteroposterior width of fossa; **57**, ectopterygoid pneumatic excavation subcircular; **58**, caudal 15 and more posterior caudals with elongate prezygapophyses; **59**, coracoid postroventral process length more than twice glenoid diameter; **60**, ischial obturator flange triangular; **61**, pubic obturator notch; **62**, femoral fourth trochanter weak or absent; **63**, fibular fossa occupying all of the medial aspet of the proximal end.
46. Supported by The David and Lucile Packard Foundation, the National Geographic Society, and The Eppley Foundation for Research. We thank C. Abraczinskas for executing the finished illustrations; Q. Cao, R. Macek, and G. Wilson for fossil preparation; M.-S. Cornier, J. Hopson, A. Milhi, and H.-D. Sues for their contributions in the field; M. Carrano, J. Hopson, and H.-D. Sues for reviewing an earlier draft of the paper; and M. Bensaïd and M. Dahmani (Ministère de l'Energie et des Mines, Rabat, Morocco) for their support of this research.

29 February 1996; accepted 3 April 1996

Lead and Helium Isotope Evidence from Oceanic Basalts for a Common Deep Source of Mantle Plumes

B. B. Hanan and D. W. Graham

Linear arrays in lead isotope space for mid-ocean ridge basalts (MORBs) converge on a single end-member component that has intermediate lead, strontium, and neodymium isotope ratios compared with the total database for oceanic island basalts (OIBs) and MORBs. The MORB data are consistent with the presence of a common mantle source region for OIBs that is sampled by mantle plumes. $^{3}He/^{4}He$ ratios for MORBs show both positive and negative correlation with the $^{206}Pb/^{204}Pb$ ratios, depending on the MORB suite. These data suggest that the common mantle source is located in the transition zone region. This region contains recycled, oceanic crustal protoliths that incorporated some continental lead before their subduction during the past 300 to 2000 million years.

Earth's mantle is geochemically heterogeneous, but the origin, scale, and distribution of chemical variations are uncertain. Analyses of oceanic basalt isotope compositions seem to indicate mixtures of at least four mantle components (*1*). Recently, another mantle component located internal to these four was identified on the basis of Sr-Nd-Pb-He isotope data (*2–4*). Trends of Pb isotope data for MORB suites converge on a position internal to the global mantle components and define a common end-member for MORBs (*5*). Here, we show that the MORB and OIB data define the same inter-

B. B. Hanan, Department of Geological Sciences, San Diego State University, San Diego, CA 92182-1020, USA.
D. W. Graham, College of Oceanic and Atmospheric Sciences, Oregon State University, Corvallis, OR 97331-5503, USA.